Environmental Science and Pollution Research
https://doi.org/10.1007/s11356-023-25319-8

RESEARCH ARTICLE

An evaluation of long-term gridded datasets of total columnar ozone retrieved from MERRA-2 and AIRS over the Indian region

Priyanshu Gupta[1] · Swagata Payra[2] · R. Bhatla[3,4] · Sunita Verma[1,4]

Received: 29 September 2022 / Accepted: 10 January 2023

Abstract

Accurately determining the spatiotemporal variability of ozone on a regional to intercontinental scale is essential for air quality studies. In the present study, a first systematic evaluation and analysis of long-term (2009–2020) gridded datasets ($0.5° \times 0.625°$) of total columnar ozone (TCO) retrieved from Modern-Era Retrospective Analysis for Research and Applications, version 2 (MERRA-2_{TCO}) is evaluated for the Indian region. The MERRA-2_{TCO} is first validated with observations (IMD_{TCO}) and then further compared with the Atmospheric Infrared Sounder ($AIRS_{TCO}$) satellite datasets. For an in-depth comparison and statistical analysis, the dataset has been segregated into seven distinct regions, i.e., Western Himalaya (WH), North East (NE), North Central (NC), North West (NW), West Peninsula India (WPI), East Peninsula India (EPI), and South Peninsula India (SPI). Descriptive statistics (NMSE, FB, R, FA2, and d) reveals a significant correlation of MERRA-2_{TCO} against IMD_{TCO} for Delhi with NMSE (0.0013), FB (−0.029) and Varanasi NMSE (0.0008), FB (−0.014). The results of simple linear regression analysis show an increasing TCO trend value of 0.31% and 0.44% per decade in both the cities, respectively. A comparison of MERRA-2_{TCO} with $AIRS_{TCO}$ shows a significant correlation of 0.62–0.87 in different regions of India. Furthermore, in support of Brewer's circulation pattern, an increasing shift of columnar ozone from low (SPI) to high (WH) latitudinal regions is observed. Our results show that the MERRA-2 ozone dataset can be effectively used for ozone air quality studies over India and this analysis may strengthen the need for independent, high-quality, and consistent ozone measurements with small uncertainties.

Keywords Total column ozone · MERRA-2 · AIRS · Air quality · Validation

Introduction

Atmospheric ozone is one of the most studied gaseous constituents, for determining the thermal structure of the atmosphere (de Forster et al. 1997) to participating in tropospheric photochemical reactions (Crutzen 1974). Ozone plays a wide role in different layers of the atmosphere. Lower tropospheric ozone is considered as a potent air pollutant exerting harmful impacts on the ecosystem, crops, and human health in the tropical regions, particularly over India (Lefohn et al. 2018; Lu et al. 2018). Being a greenhouse gas, ozone is capable of inducing alterations in the energy balance near the Earth's surface and in tropospheric layer (McFarlane 2008). The upper tropical stratosphere and the lower latitudes are the zones receiving the strongest UV radiations across the globe and hence are the region producing the major amount of atmospheric ozone.

An important parameter used by the scientific community to quantify the variation in ambient ozone concentration is the total column ozone (TCO). TCO can be defined as the total concentration of ozone present in a vertical air column having a 1 cm^2 base area, at standard pressure and temperature. About 90% of this total columnar ozone is stratospheric ozone which is responsible for absorbing

Responsible Editor: Gerhard Lammel

✉ Sunita Verma
verma.sunita@gmail.com

[1] Institute of Environment and Sustainable Development, Banaras Hindu University, Varanasi, Uttar Pradesh, India

[2] Department of Remote Sensing, Birla Institute of Technology Mesra, Ranchi, Jharkhand, India

[3] Department of Geophysics, Banaras Hindu University, Varanasi, Uttar Pradesh, India

[4] DST-Mahamana Centre of Excellence in Climate Change Research, Banaras Hindu University, Varanasi, Uttar Pradesh, India

Published online: 20 January 2023

the solar ultraviolet radiation (de Forster et al. 1997). Around the year, the peak TCO values are reported in the mid-latitude and polar regions of the world except during the ozone hole period. Since the 1990s, positive trends were reported for global TCO, majorly resulting due to the implementation of the Montreal Protocol along with its amendments to curb ozone-depleting substances (ODS) emissions (Salby et al. 2011; Chipperfield et al. 2017). Using satellite-retrieved data and Dobson spectrophotometer, climatological mean TCO values have been reported to be 275.02 ± 6.44 (New Delhi), 269.03 ± 7.34 (Varanasi), 260.78 ± 5.07(Pune), and 258.71 ± 6.36 DU (Kodaikanal) respectively for the period 1957–2015 and a significant increasing trend in TCO seen over Pune, New Delhi, and Kodaikanal (Pathakoti et al. 2021). Several authors studied ozone distribution and evaluation over the India region (Londhe et al. 2003; Sahoo et al. 2005; Tandon and attri 2011; Resmi et al. 2020). Chakrabarty et al. (1998) validated the TCO against ground-based Dobson spectrophotometer measurements for six stations from 1957 to 1996 (23–45 years) and reported a negative trend in TCO at all stations except Varanasi.

The aforementioned results reveal that large variability exists in the spatio-temporal distribution of total columnar ozone; thus, present analysis may strengthen the need for independent, high-quality, consistent, and long-term global measurement with small uncertainties. One of the key components to better understand the historical events and for validating models projecting future changes is utilizing good-quality ozone datasets. Additionally, quantifying trends and variability of ozone will also require the same. This is particularly important over the tropical region which covers a large fraction of the world and experiences upper troposphere to lower stratosphere exchange (Monahan et al. 2007). However, the availability of long-term ozone data sets with high resolution is sparse with only a handful meeting all the prerequisites.

In this regard, useful observations can be acquired from space-borne instruments in order to achieve the required spatio-temporal coverage. For the estimation, the TCO dataset can be acquired from sensors onboard polar-orbiting satellites. A few examples of such sensors are global ozone monitoring experiment (GOME), microwave limb sounder (MLS), ozone monitoring instrument (OMI), total ozone mapping spectrometer (TOMS), scanning imaging absorption spectrometer for atmospheric chartography (SCIAMACHY), etc. Among this one, particularly useful high-quality observations are provided by AIRS, launched in the year 2002, and are being utilized for monitoring global ozone variability and trends over a decade (Monahan et al. 2007). Nonetheless, these instruments can only aid in understanding the global variability of the ozone and geographical or vertical distribution with limited temporal coverage.

To combat this setback, atmospheric reanalysis datasets were developed which produces long-term global records of atmospheric composition and meteorological fields with a high spatial and temporal resolution by employing the data assimilation methodology (Cohn 1997; Kalnay 2003) whereby ground-based observations and satellite-retrieved dataset are merged with general circulation model (GCM) simulations. In 2009, NASA's Global Modelling and Assimilation Office (GMAO) was the first released Modern-Era Retrospective Analysis for Research and Applications (MERRA-2), a reanalysis dataset created using the Goddard Earth Observing System (GEOS) data assimilation system (DAS) covering the time period of 1979–2015. The accent of this paper particularly falls on MERRA-2 dataset (Bosilovich et al. 2015) which trailed the aforementioned reanalysis.

While the majority of the reanalysis incorporates assimilated ozone fields, the widespread utilization of these datasets in scientific investigations is still lacking, primarily due to the uncertain quality of these fields and the overall lack of validation. Instead, scientists choose to make use of ground-based and satellite-retrieved ozone datasets alongside assimilated climatological parameters.

Therefore, the focus of the present work is to fully analyze the TCO product from MERRA-2 regarding biases, random errors, and long-term constancy with respect to ground-based TCO observations. In this context, the accuracy and long-term stability of total column ozone estimates from the MERRA-2 product will be examined via comparisons to already established spaceborne mission atmospheric infrared sounder (AIRS) on NASA's aqua satellite, which have been collocated in space and time. Hence depending on the data availability, this study validates MERRA-2 columnar ozone with IMD observe datasets over New Delhi and Varanasi cities for a long-term period. Another objective is to compare MERRA-2 and AIRS products to determine monthly, annual, and seasonal variations of TCO datasets over selected regions of India, i.e., WH, NE, NW, NC, WPI, EPI, and SPI.

The paper is organized as follows. The "Materials and methods" section describes the dataset and different statistical methodology used for the analysis. In the "Results" section, we present the comparative results of the total column ozone dataset, their associated bias, and errors. The conclusion and summary are drawn in the "Discussion and conclusion" section.

Materials and methods

The area of study has a latitudinal extent of 7°N to 38°N with a longitudinal range of 65°E to 99°E. It covers all the significant geographic features, such as the Himalayan Mountain Region, Indo-Gangetic plains, deserts, and coastal regions,

except the oceanic region in the Indian subcontinent. For an in-depth comparison and statistical analysis, the dataset has then been segregated into seven distinct regions following IITM criteria (Gupta et al. 2020), i.e., Western Himalaya (WH), Northeast (NE), North Central (NC), Northwest (NW), West Peninsula India (WPI), East Peninsula India (EPI), and South Peninsula India (SPI) as shown in Fig. 1.

Dataset description

The total columnar ozone dataset has been collected for Indian subcontinent regions from AIRS and MERRA-2 during 12-year (2009 to 2020) period.

AIRS

The atmospheric infrared sounder (AIRS) launched in 2002 aboard NASA/Aqua satellite, crosses the equator at approximately 13:15 LST (Aumann et al. 2003). The apparatus provides near-global coverage two times in a day with a swath of 1650 km. The AIRS instrumental suite comprises of atmospheric infrared sounder (AIRS), advanced microwave sounding unit (AMSU-A1 and AMSU-A2), and humidity sounder for Brazil (HSB). AIRS is a grating spectrometer whose radiance spectra are utilized in determining the vertical profile of trace gases (water vapor, ozone, carbon monoxide, and methane) and temperature along with surface and cloud

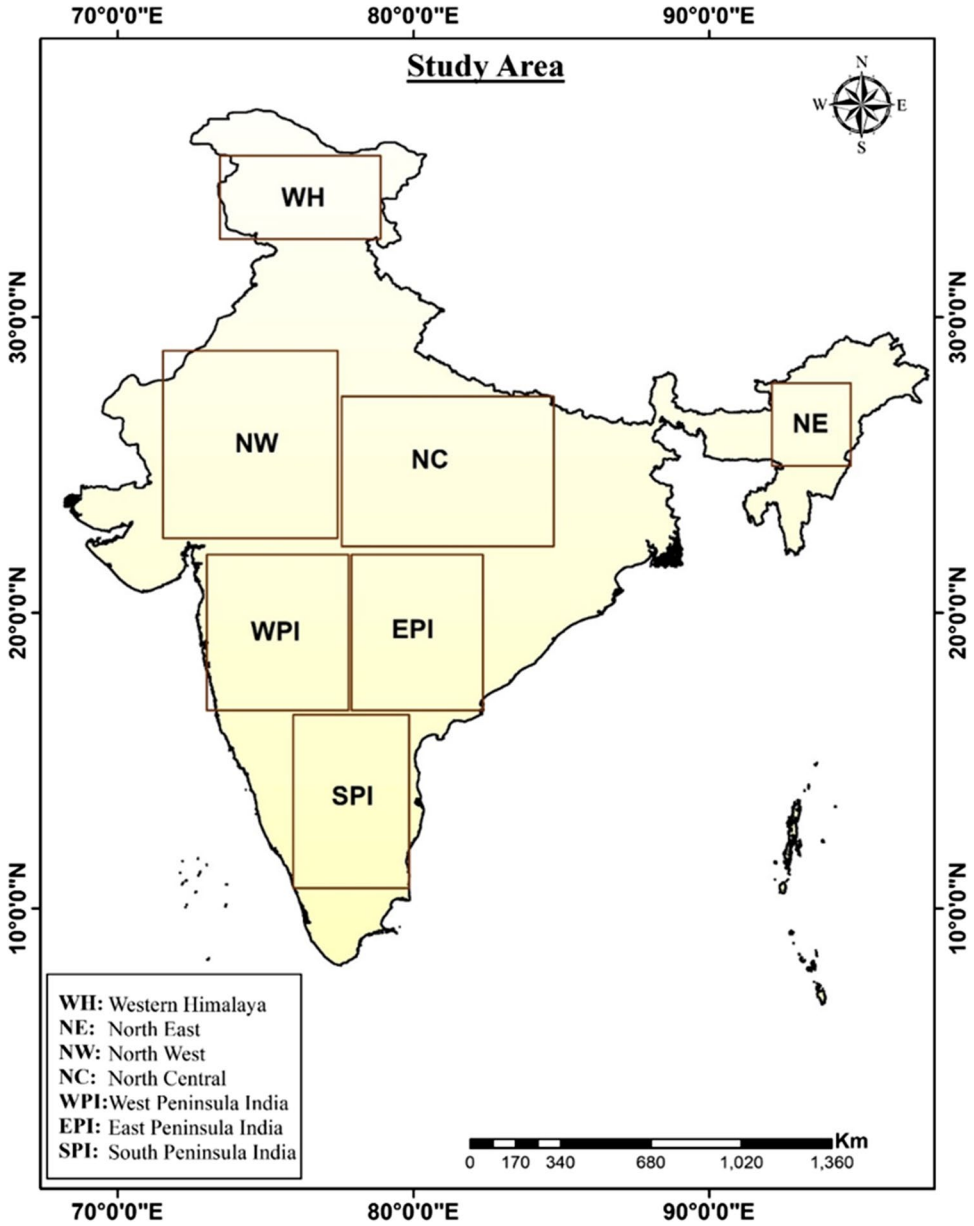

Fig. 1 Study area map representing India and its different regions

properties. The AIRS sensor has four absorption channels in the visible wavelength range of 0.4–1.0 μm and 2378 absorption channels in the infrared (IR) wavelength range of 3.75–15.4 μm (https://airs.jpl.nasa.gov/mission/overview/). Additionally, the advanced microwave sounding unit-A (AMSU-A) device onboard the Aqua satellite has 15 microwaves (MW). Calculation of TCO values was achieved by merging the observed radiations in IR/MW wavelength, grounded on ascending (day) and descending (night) monitoring (Kim et al. 2021). Divakarla et al. (2008) validated the AIRS V4 and V5 algorithm total ozone amounts against global BD station and found a well-matched measurement with an RMS difference of 8% and bias of less than 4%. However, AIRS level-2 version-6 products produced at the Goddard DISC near real time have significant advancement in their retrieval algorithm compared to previously used version 5. The most important improvement is the physical retrieval methodology which determines information about surface spectral emissivity and surface skin temperature using cloud-cleared radiances in the shortwave window region of 2396 and 2664 cm^{-1} (Susskind et al. 2006), resulting in an upgradation in the quality of both land and ocean surface skin parameters during day and night time conditions. In the current study, we have used Level 2, V006 AIRS retrieved datasets (AIRS/Aqua L2 Standard Physical Retrieval, (AIRS2RET006) with a spatial resolution of 50 km × 50 km. It consists of the retrieved temperature profile, carbon monoxide, ozone, water vapor, and methane as well as retrieval estimates of cloud and surface properties. AIRS-only (AO) version-6 retrieve mode generated good results as those of the full AIRS/AMSU mode (Susskind et al. 2011). In this product, 6 min of AIRS granules has been set with 30 footprints cross track by 45 lines along the track. A total of 240 granules per day are there, approximately with an orbit repeat cycle of 16 days.

MERRA-2

Providing a dataset from the beginning of 1980, Modern-Era Retrospective analysis for Research and Applications, Version 2 (MERRA-2) was introduced as a successor to the original MERRA dataset. Advancements were made in the assimilation system that enables the assimilation of microwave observations and hyperspectral radiances. The important component of the MERRA-2 model was the improvement in the grid point statistical interpolation analysis scheme (Kleist et al. 2009) and the Goddard Earth Observing System atmospheric model. NASA's AURA MLS ozone profile observations were also taken into account from late 2004. Wargan et al. (2015) reported the good agreement of MERRA-2_{TCO} against the ozonesonde in the lower stratosphere. The dataset is provided at a grid resolution of 0.5° × 0.625°. MERRA-2 columnar ozone is available at 1 h, 3 h, and monthly temporal resolution. This study uses the MERRA-2 (M2T1NXCHM_5.12.4) 1-h columnar ozone for time period 2009–2020.

IMD observations

Dobson spectrophotometer is used to measure TCO and is monitored by India Meteorological Department (IMD) at New Delhi, Varanasi, Ahmedabad, Pune, Dum Dum, Kodaikanal, Mount Abu, and Srinagar stations. Observed daily TCO datasets for the study regions are acquired from the Dobson spectrophotometer and maintained by IMD. The Dobson spectrophotometer instrument is established in the early 1920s. It is based on the intensity measurement principal of ozone-attenuated radiation in a number of narrow spectral bands. Dobson spectrophotometers play an important role in monitoring the total column ozone (Komhyr and Evans 1980; Komhyr et al. 1989). The reliability and accuracy of the Dobson spectrophotometer for different Indian stations have been discussed by Chakrabarty and Peshin (1997). India Meteorological Department (IMD) has performed a widespread inter sensor calibration with the Dobson spectrophotometer network (Chakrabarty et al. 1998). Depending on data availability this paper utilizes ground-based TCO of New Delhi and Varanasi cities for time period of 2009–2018.

Methodology

The columnar ozone of MERRA-2 reanalysis product (https://gmao.gsfc.nasa.gov/reanalysis/MERRA-2/data_access/) for the period 2009–2018 is validated against the observed data from Indian Metrological Department (IMD). It can also be accessed from World Ozone and Ultraviolet Radiation Data Centre (WMO-GAW/WOUDC; http://www.woudc.org) over New Delhi and Varanasi city. Furthermore, for the comparative study, MERRA-2 at 0.5 × 0.625 grid resolution and AIRS retrieved datasets (AIRS/Aqua L2 Standard Physical Retrieval (AIRS-only) (AIRS2RET 006) with spatial resolution 50 km × 50 km have been extracted over the different regions in India. Since, AIRS passes through the equator at 13:30 LT in its descending and ascending orbit. While for MERRA-2, TCO data are available in every 1 h. Hence both the datasets at 1:30 local time period have been taken to compare the MERRA-2 and AIRS TCO products. Furthermore, for the best grid matches, AIRS datasets (0.5 × 0.5) have been extrapolated to MERRA-2 (0.5 × 0.625) spatial grid, and analysis has been performed on a daily, monthly, annual, and seasonal basis. The details of comparison statistics can be found in Appendix 1.

Results

In the present section, MERRA-2 columnar ozone has been compared with ground-based TCO for the period 2009–2018 over the Indian cities.

Evaluation of MERRA-2_{TCO} against IMD_{TCO}

The monthly mean (2009–2018) variation of columnar ozone acquired from MERRA-2 and IMD over Delhi and Varanasi cities is depicted in Fig. 2. Both datasets follow the same pattern of TCO variation, with underestimation of MERRA-2_{TCO} with respect to IMD_{TCO}. Maximum columnar ozone is noted in the months of March, April, May, and June, with TCO values of 300DU and 280DU for Delhi and Varanasi cities respectively. It might be linked to higher photochemical production due to high temperatures in summer. Additionally, a reduction in TCO concentration is observed in both cities from June to December as a result of an increase in cloud cover, heavy monsoon rainfall, and cooler temperatures. In addition, the long-term decadal TCO trend in both the cities from 2009 to 2018 is also examined using the SLR technique. In Delhi and Varanasi, respectively, a positive TCO trend value of 0.31% and 0.44% per decade is seen. An increase in anthropogenic activity may be the cause of this rising pattern. Due to anthropogenic activities, the combustion of fossil fuels in automobiles and stationary power plants has increased nitrogen oxide and volatile organics emissions into our atmosphere. Nitrogen oxides and hydrocarbons interact in sunlight, generating a rise in tropospheric ozone.

Descriptive statistical analysis

In order to compare columnar ozone of a reanalysis product (MERRA-2) with observed TCO datasets of IMD, several descriptive statistics like normalized mean square error (NMSE), fractional bias (FB), correlation coefficient (R), factor of two (FA2), and index of agreement (d) have been used for monthly mean datasets of Delhi and Varanasi cities (Table 1). The normalized discrepancy value in the entire dataset is highlighted by the NMSE.

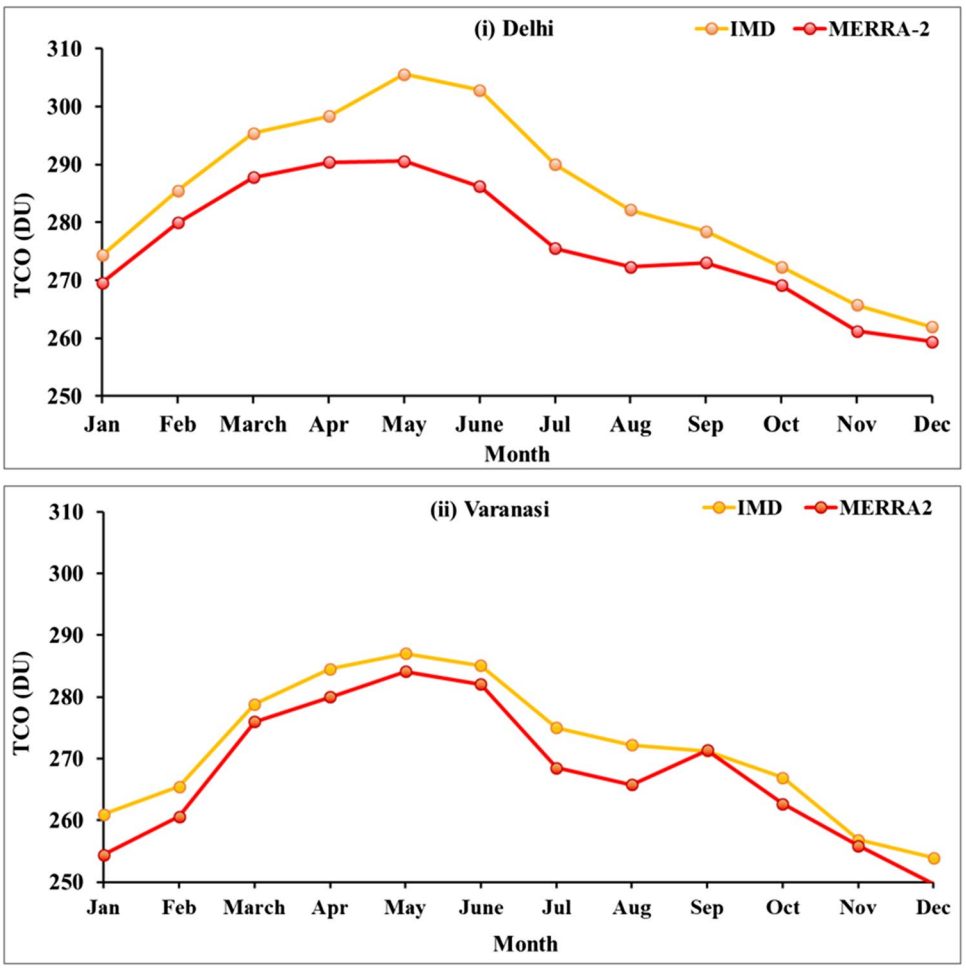

Fig. 2 Monthly mean TCO of MERRA-2 and IMD observed during 2009–2018 for (i) Delhi and (ii) Varanasi city

Table 1 Descriptive statistical analysis of MERRA-2 columnar ozone against the observation datasets

Statistics	MERRA-2 Vs. IMD	
	Delhi	Varanasi
NMSE	0.00134	0.00082
R	0.94	0.88
FB	−0.029	−0.0145
FA2	100	100
D	0.88	0.91

Over Delhi and Varanasi, lower NMSE values of 0.0013 DU and 0.00082 DU were observed, indicating that the MERRA-2 product is performing more adequately. Additionally, FB has been calculated to assess whether datasets have been overestimated or underestimated. A reanalysis of MERRA-2 against observation data in Delhi and Varanasi shows FB of − 0.029 and − 0.0145, respectively. Comparatively, low FB and NMSE values of MERRA-2 columnar ozone reflect good quality of TCO data specially for Varanasi city. The factor of two or FA2 has also been studied. The percentage of predictions that are within a factor of two of the observed values is indicated by that. An FA2 value of 100% is reached in both stations, which satisfies the ideal value requirements. R and d, another significant statistical measure, shows a strong correlation between the datasets of the two cities. Delhi and Varanasi reported 0.94 and 0.88 R values, indicating how much the two TCO products correlate or move together, and 0.87 and 0.91 d values, showing how much the means and variances of the IMD and MERRA-2_{TCO} differ additively and proportionally (Legates and McCabe 1999).

Furthermore, The ECDF plot of MERRA-2 and IMD over Delhi and Varanasi from 2009 to 2018 is shown in Fig. 3 i and ii. An ECDF is an estimator of the cumulative distribution function. It denotes the number of observations in a collection that are below each distinct value. In order to determine whether the entire feature is spread across the data set, a sequence of data from least to greatest has been shown. Over Delhi, there is a strong correlation between MERRA-2 data and IMD in both the lower and upper TCO value distributions. In the 210–250 DU range, 1–20% of TCO was dispersed, and larger amounts were spread up to 310–350 DU. Between 25 and 90% of the TCO distribution, or between 270 and 300 DU, there is a difference between both datasets. Comparing MERRA-2_{TCO} to the IMD recorded in Delhi city, we find that it is generally underestimated. In contrast, both datasets in Varanasi showed a strong correlation across the entire TCO distribution, with only a slight discrepancy in 230–270 DU lying between 10 and 40% of the TCO. Overall, MERRA-2_{TCO} values are underestimated by the IMD over the Varanasi station. Additionally, the boxplot also reveals that for both cities, the columnar ozone of observed datasets is

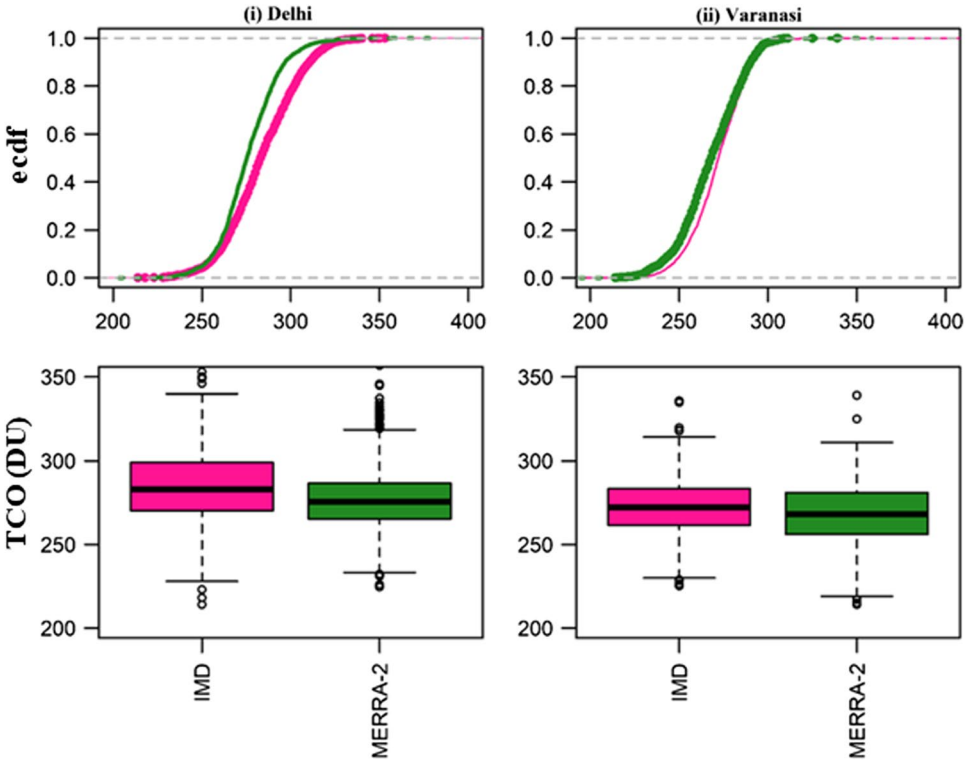

Fig. 3 ECDF plot of MERRA-2_{TCO} and IMD_{TCO} over Delhi and Varanasi city for time period of 2009–2018

spreading more widely and has a higher range of TCO value than the columnar ozone of MERRA-2.

Comparative assessment of MERRA-2_{TCO} with $AIRS_{TCO}$

Spatial variation of annual and seasonal mean TCO

A spatial comparison of MERRA-2 and AIRS satellite products has been explained annually and seasonally from 2009 to 2020 after analyzing the MERRA-2_{TCO} product with respect to observation datasets.

Distributions of annual mean TCO shown in Fig. 4 indicate a similar pattern in both datasets, with TCO values ranging from 270 to 284 DU in northern regions (WH, NE, NW, and NC) and 260 to 274 DU throughout the southern Indian regions (WPI, EPI, and SPI). TCO is found to have a robust increasing pattern from low to high latitudinal locations. Additionally, a comparison of these two products shows an overestimation of $MERRA2_{TCO}$ by 2DU for the northern and central regions of India and an underestimation by 4DU to 1DU over most of the southern regions. Particularly in WPI, TCO values for MERRA-2 range from − 8 to − 1 DU, which indicates a significant degree of underestimation. Fluctuations in these atmospheric ozone distributions are caused by chemical and dynamical phenomena (Randel 1988; Shepherd 2008; Mcconnell and Jin 2008). One of the key factors that contribute to a greater TCO in the middle to high latitudes is the Brewer-Dobson circulation (Fioletov 2008; Shepherd 2008; Butchart

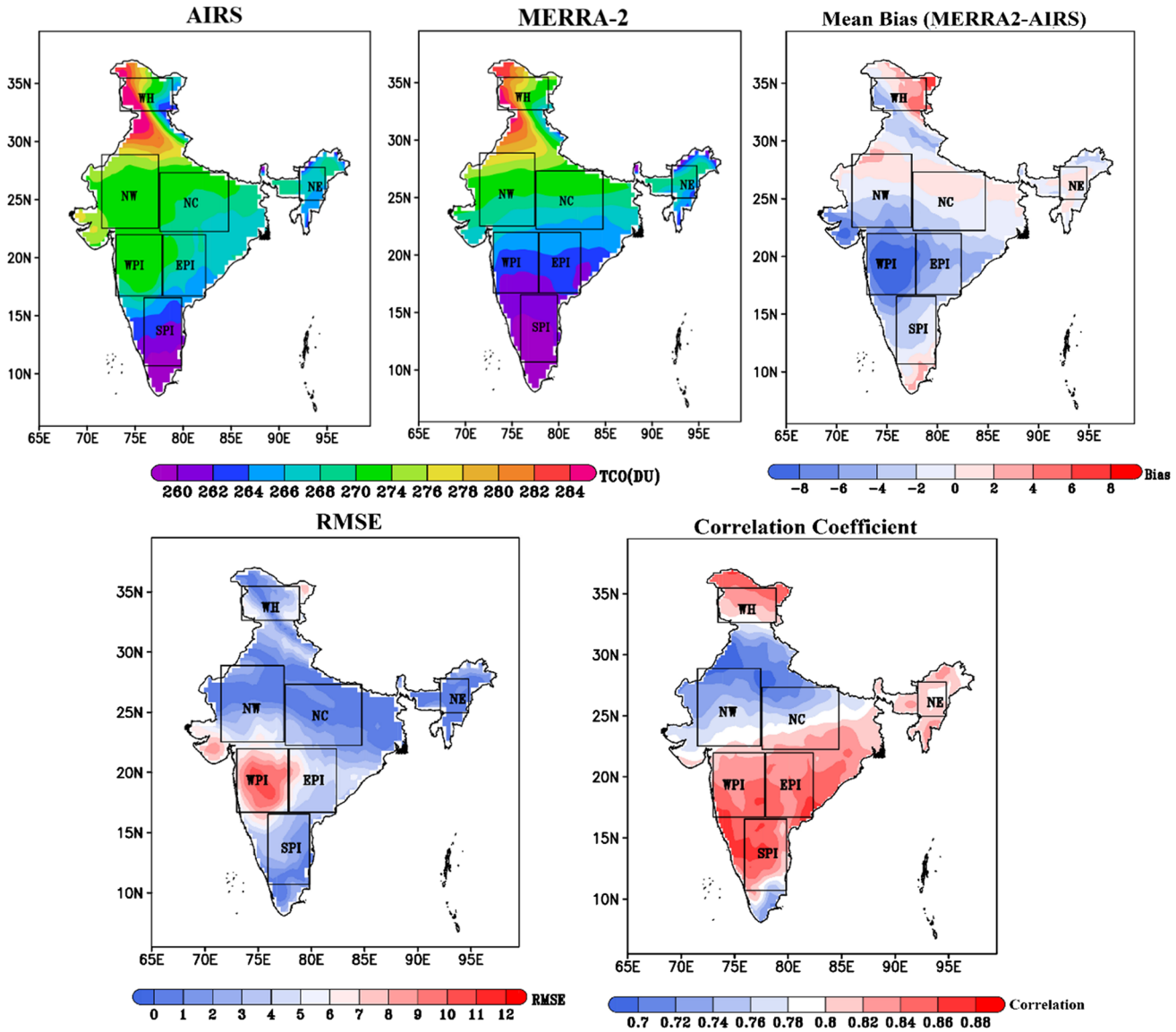

Fig. 4 Spatial variation of annual mean TCO derived from MERRA-2 and AIRS datasets during time period of 2009–2020

2014). Brewer (1949) and Weber et al. (2011) suggest that it is the stratospheric global-scale air circulation, which is characterized by air upsurges in low-latitude regions, poleward motion, and subsequent descent in the middle and high latitudes. TCO in this context, according to both MERRA-2 and AIRS, also denotes a high concentration toward higher and middle latitudinal regions. The TCO in WH, NW, and NC is between 270 and 284 DU, with a mean bias of 1 DU. In contrast, low latitudes, such as the southern part of India (EPI, WPI, and SPI), show a low distribution of TCO (260–274 DU for AIRS and 260–266 DU for MERRA-2), indicating an underestimating of MERRA-2 TCO by − 4 to − 1 DU. Overall, the largest mean bias (− 8 DU) between the two datasets is seen throughout all of the WPI regions, with an RMSE value of 102 DU. With correlation values of 0.80–0.88 in the northern and southern regions, $MERRA2_{TCO}$ and $AIRS_{TCO}$ show a strong agreement, although a moderate correlation coefficient (0.7–0.78) is seen in the middle region.

Seasonal variations of mean TCO retrieved from AIRS and MERRA-2 have been spatially depicted in Fig. 5. Analysis has been performed for the winter (DJF), pre-monsoon (MAM), monsoon (JJAS), and post-monsoon (ON) season. Though columnar ozone is well distributed by both the products, depending on seasons, they slightly differ from each other. Based on different meteorological and topographical patterns, India has been divided into seven different regions, i.e., WH, NE, NW, NC, EPI, WPI, and SPI. Therefore, the TCO pattern may show significant variability according to different seasons and regions. Figure 5a shows the spatial distribution of TCO during the winter season. In winter, $MERRA\text{-}2_{TCO}$ and $AIRS_{TCO}$ lie between 246 and 290 DU. Both products agree well in the WH region, with TCO values ranging from 274 to 290 DU and a mean bias of 2 DU. MERRA-2 is overestimated by AIRS in the NW, NC, and NE regions, with a mean bias of + 1 to + 8 DU, and TCO varies between 250 and 262 DU. During the winter season, the prevailing wind speed is low, and thus, stability is high; additionally, because it is an industrial and densely populated area, pollutants are emitted in greater quantities, and these are trapped. The high ozone value of MERRA-2 product may be due to the contribution of emission inventory specially over the IGP region (Ziemke et al. 2019). In the WPI region, TCO varies from 250 to 258 DU (AIRS) and (242–254 DU) in MERRA-2 with a mean bias of − 8 to − 3 DU. While in the EPI and SPI regions, both the datasets show the same pattern (242–248 DU) with a mean bias of − 4 to − 1 DU.

MERRA-2 and AIRS products (266–290 DU) show high TCO concentrations during the pre-monsoon season (Fig. 5b). Summer TCO values are higher due to the high photochemical production of ozone during this season. The summer month experiences higher solar radiation, temperature, and sunshine duration compared to other seasons (Soni et al. 2012). During this season, both the products follow the same spatial pattern with a slight difference in WPI (− 4 to − 6 DU), upper NW, WH, and NE regions (4DU).

TCO concentrations in range of 254 to 290 DU (AIRS) and 262 to 282 DU (MERRA-2) are seen during the monsoon season (Fig. 5c). In this season, MERRA-2 undergoes underestimation almost over all of India with a mean bias of − 8 to − 1 DU. These significant bias results from the fact that MERRA-2 is an all-sky product, but AIRS, an infrared sensor, has a cloud filtering algorithm and does not take into account all cloudy scenarios. Though many factors cause the low tropospheric ozone during the monsoon season (Lal et al. 2013; Lu et al. 2018), like thick cloud covers that reduce UV radiation and lead to less net chemical production of ozone, south-westerly winds dominate and bring pristine marine air masses during the monsoon season. TCO ranged between 250 and 278 DU (AIRS) and 254 and 278 DU (MERRA-2) post-monsoon (Fig. 5d). During this season, TCO remains moderate in almost all of the regions. AIRS reveals the maximum TCO concentration in the WPI region. MERRA-2 undergoes underestimation (− 7 to − 1 DU) almost in entire India.

Correlation analysis of $MERRA\text{-}2_{TCO}$ and $AIRS_{TCO}$

Figure 6 presents the density scatter plot of MERRA-2 and AIRS daily columnar ozone for seven different regions (WH, NE, NW, NC, EPI, WPI, and SPI) in India during 2009–2020. The red dots correspond to regions with high densities of samples, and the dark blue to very low densities of samples. The performance of MERRA-2 columnar ozone is evaluated based on various statistics, like the following: NMSE, R, FB, FA2, and d against the AIRS datasets. This analysis suggests that $MERRA\text{-}2_{TCO}$ is showing good agreement with $AIRS_{TCO}$ datasets for almost all the regions with low NMSE, FB, and high R statistics. All seven regions show a significant correlation with AIRS data and a low mean bias. The values of various statistical variables shown in Table 2 and Fig. 6 show that the WH region has the best overall validation metrics with R (0.87), FB (0.05), NMSE (0.0047), and d (0.86), followed by the NE regions with R (0.78), bias (0.021), NMSE (0.0029), and d of 0.85.

Monthly variation in Total column ozone

Figure 7 shows the monthly average TCO (2009–2020) retrieved from MERRA-2 and AIRS datasets over the study region. All the regions (NE, NW, NC, EPI, WPI,

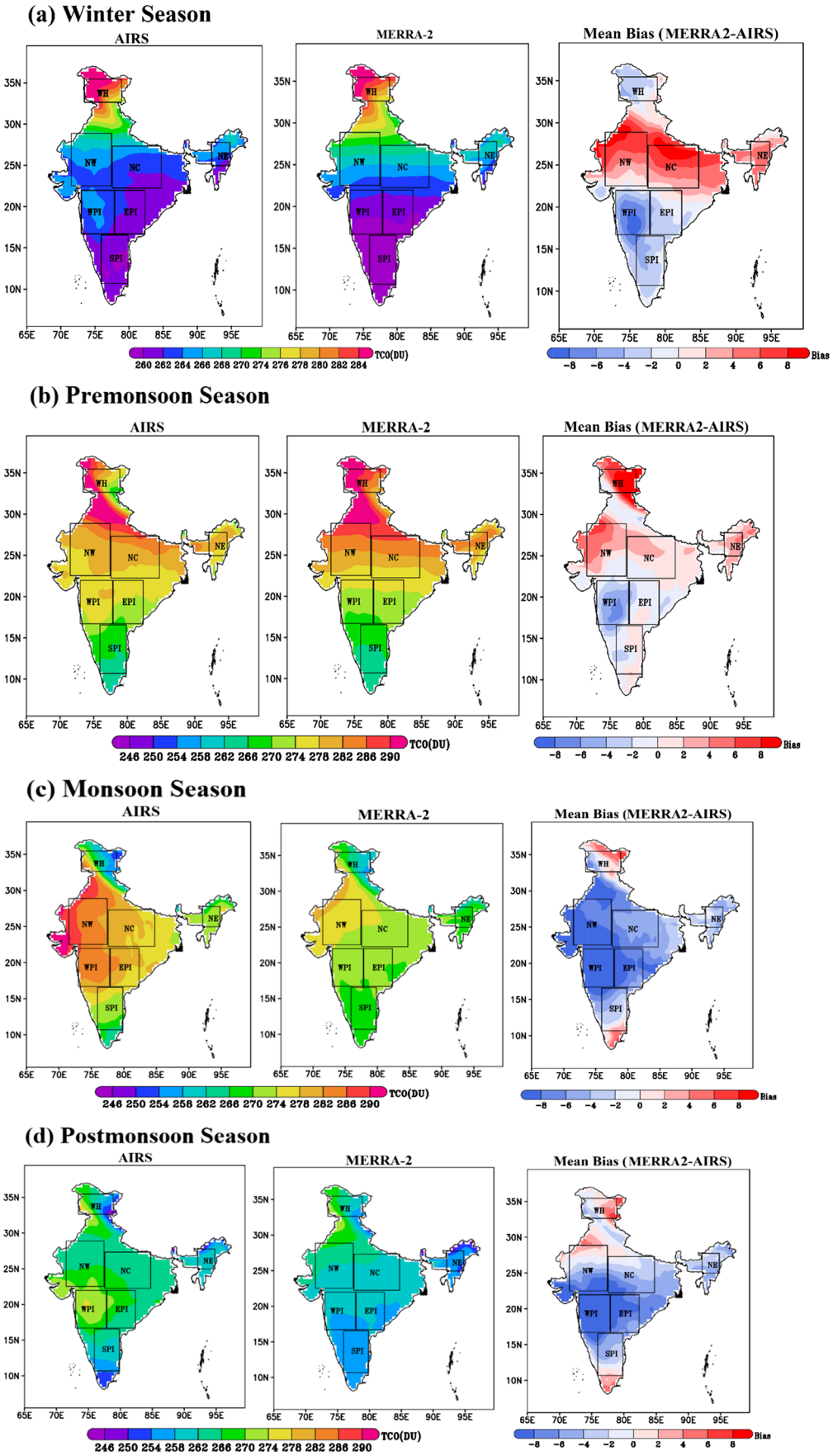

Fig. 5 Seasonal distributions; **a** winter, **b** Pre-monsoon, **c** monsoon, and **d** post-monsoon season of MERRA-2 and $AIRS_{TCO}$ during 2009–2020

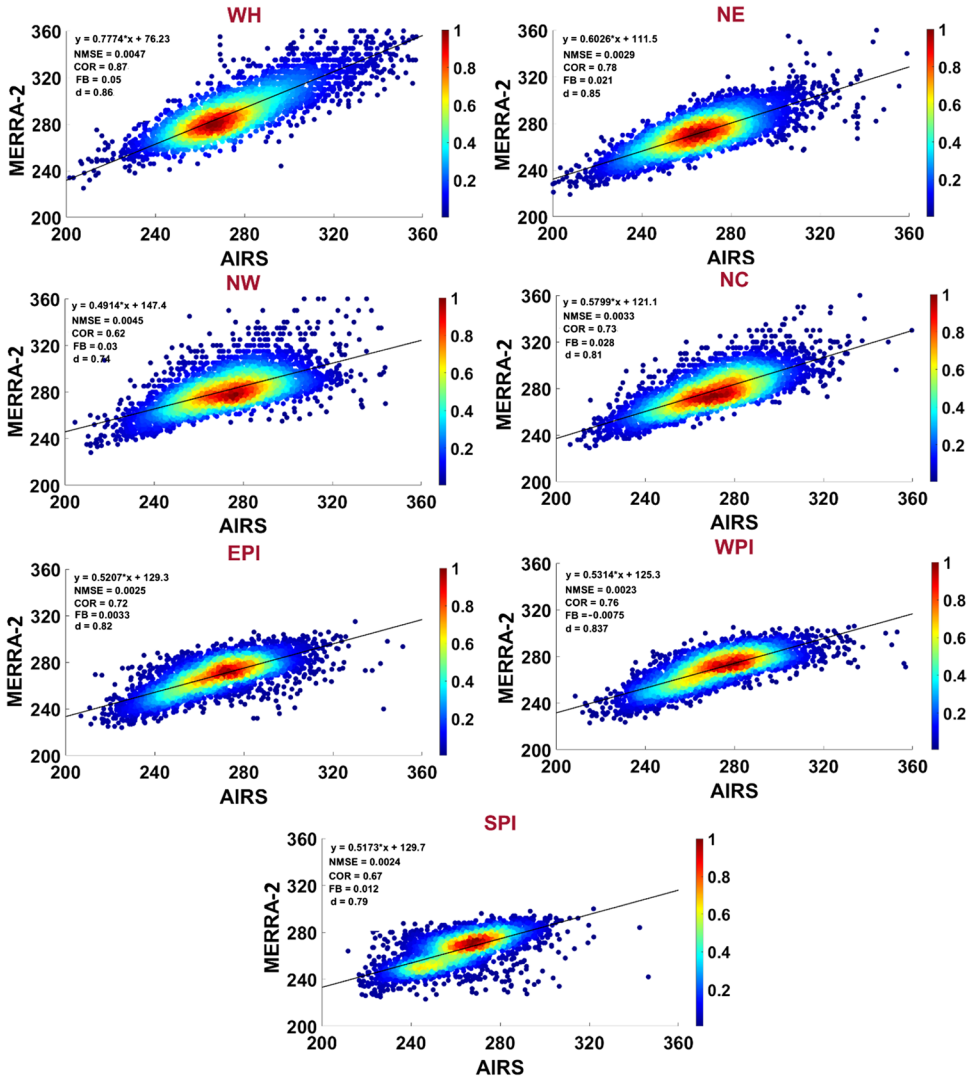

Fig. 6 Density scatter plot, comparing MERRA-2 and AIRS TCO over different regions of India

and SPI) except WH reveal maximum TCO concentration during the summer months, i.e., March, April, and May months. Maximum TCO in the WH region is seen during the months of January, February, and March, ranging from 291 to 305 DU (AIRS) and 305 to 315 DU (MERRA-2). In northern India, Resmi et al. (2020) also reported maximum TCO during the February and March months. Ozone transport from tropical to extratropical regions is dominant during the winter (Fioletov 2008), and it is the primary reason for the annual maximum toward higher latitudes than the tropics. It has been seen that in the NE, NW, NC, EPI, WPI, and SPI regions, maximum average TCO values are seen in the months of March, April, May, and June, which are accompanied by high temperatures, sunshine hours, and low humidity, followed by monsoon months. A slight decrease in TCO concentrations is observed from July to November throughout the regions. Furthermore, the concentration of TCO in the whole region (except WH) was found to be very low during the months of November and January, which is accompanied by low photochemical production. Then a rising trend was observed from December to March. In addition, this figure also shows a month-wise comparison of MERRA-2_{TCO} and $AIRS_{TCO}$, which fluctuate with different regions and months. During the WH and SPI regions, MERRA-2_{TCO} undergoes overestimation

Table 2 Statistical performances of MERRA-2_{TCO} and $AIRS_{TCO}$ in different regions of India

Regions	NMSE	FB	R	D
WH	0.0047	0.05	0.87	0.86
NE	0.0029	0.021	0.78	0.85
NW	0.0045	0.03	0.62	0.74
NC	0.0033	0.028	0.73	0.81
WPI	0.0023	−0.075	0.76	0.84
EPI	0.0025	0.0033	0.72	0.82
SPI	0.0024	0.012	0.67	0.79

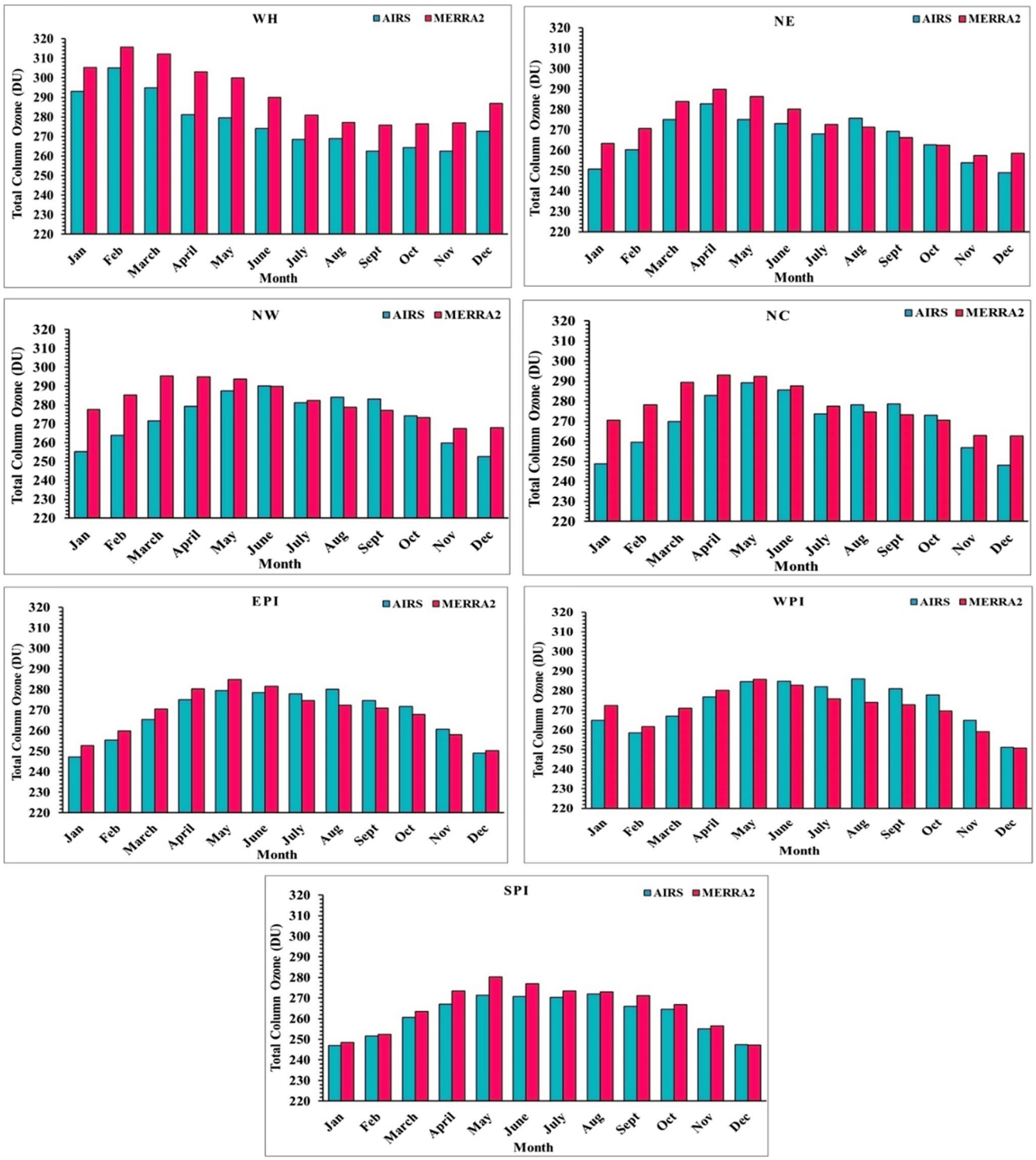

Fig. 7 Monthly average variations of $MERRA2_{TCO}$ and $AIRS_{TCO}$ in WH, NE, NW, NC, WPI, EPI, and SPI region from 2009 to 2020

during all the months. While in the NE region, $AIRS_{TCO}$ overestimated in August and September. Furthermore, in the NW, NC, EPI, and WPI regions, $AIRS_{TCO}$ is comparatively high during July, August, September, October, and November months.

Annual variation of total columnar ozone

The annual mean TCO acquired from the AIRS satellite and MERRA-2 reanalysis datasets is shown in Fig. 8. Annual trends are examined over seven different regions

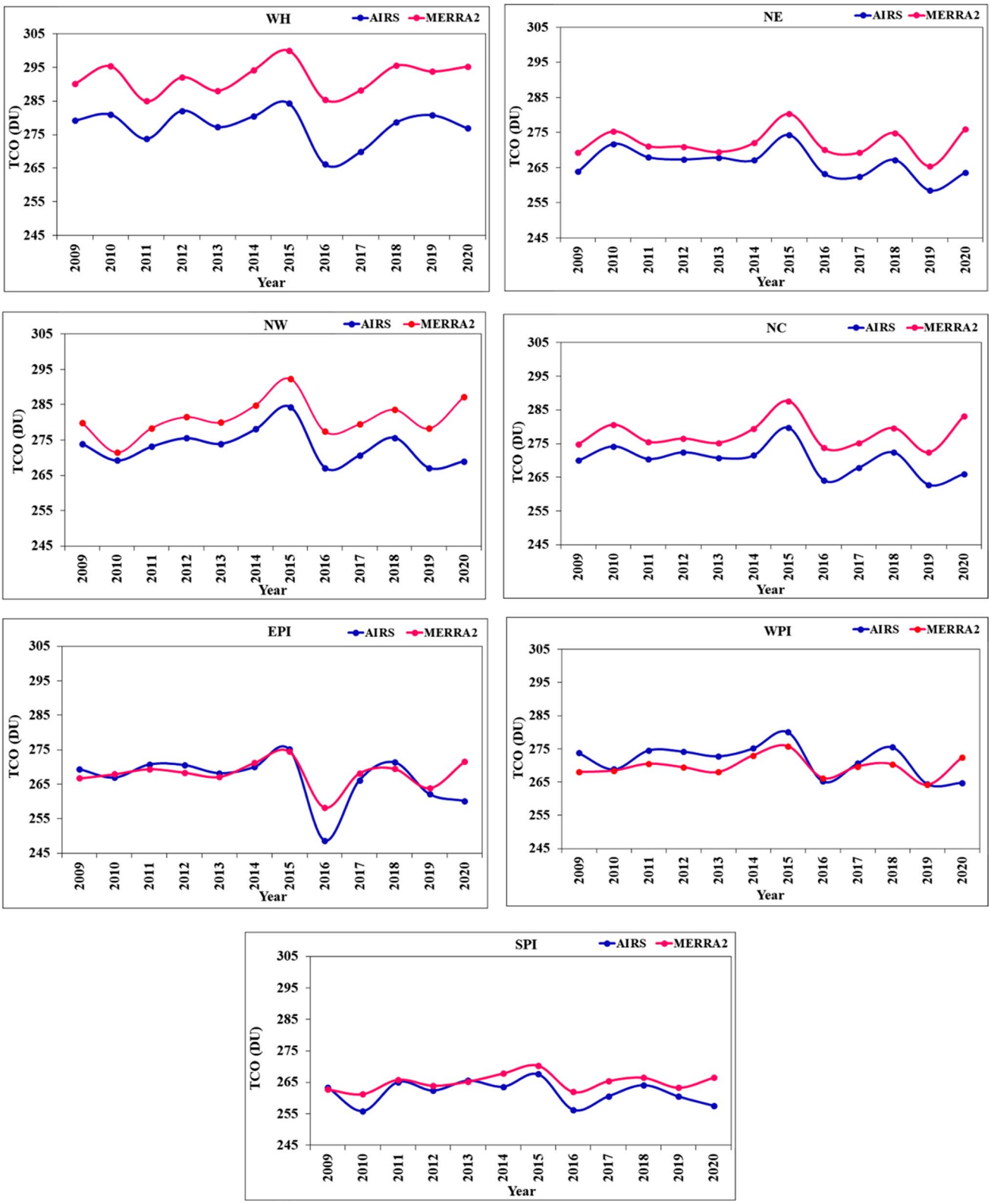

Fig. 8 Annual variation of columnar ozone from 2009 to 2020 over WH, NE, NW, NC, WPI, EPI, and SPI region

of India for the period 2009–2020. In the WH region, TCO values in the range of 266–284 DU and 285–300 DU are observed for AIRS and MERRA-2 products. Both the datasets follow the same pattern, the minimum value is seen in the year 2016, while the maximum is in 2015. In the NE region, TCO that lies in the range of 258–274.8 DU(AIRS) and 265.5–280.4 DU (MERRA-2) reported maximum column ozone in the year 2015 and minimum in 2019. NW also recorded maximum TCO in the year 2015, AIRS (284 DU) and MERRA-2(292 DU), while minimum values are reported 267DU (2016) and 271.56 DU (2010) for AIRS and MERRA-2 respectively. Similarly, in the NC region, both datasets follow the same trend with minimum and maximum values of 263 DU and 272–288 DU in the years 2015 and 2019 respectively. However, in the EPI region, both the datasets are well matched with a range of 249–275 DU(AIRS) and 258–274 DU (MERRA-2). WPI recorded a maximum TCO (280 DU and 270 DU) in the year 2015 for both datasets. Among all the regions, low columnar ozone is obtained for SPI region up to 268 DU (AIRS) and 270 DU (MERRA-2). Overall, the columnar ozone of AIRS and MERRA-2 follows the same trend in each region. In the northern parts of India (WH, NE, NW, and NC), both products follow a similar trend, where MERRA-2 is overestimated almost over all the regions. Whereas the peninsular region (EPI, WPI, and SPI) exhibits minimum bias between the datasets. Interestingly, all regions recorded high TCO (DU) in the year 2015 that may be driven by the high temperature, leading to heat wave occurrence and variation in ENSO and quasi-biennial oscillation (QBO) pattern. Global/Regional temperatures in 2015 were the highest on record, owing in part to the El Nino phenomenon. Based on an investigation of satellite ozone observation and atmospheric circulation data, Han et al. (2001) explored the ENSO signal in the interannual variation of total ozone over Tibet. They discovered that ozone levels over Tibet rise during El Nino episodes and fall during La Nina events.

Taylor diagram of seasonal mean TCO analysis

The Taylor plot shown in Fig. 9 represents the seasonal variations of mean TCO retrieved from MERRA-2 and AIRS datasets. Green, yellow, red, and blue circles represent the DJF, MAM, JJAS, and ON seasons. It quantifies the similarity between two datasets in terms of their standard deviation (SD), correlation coefficient, and centered root mean square difference (RMSD). The RMS (shown by the green contour) between MERRA-2 and $AIRS_{TCO}$ is proportional to the distance of the square sign on the *x*-axis remark as a reference value, while the radial distance from the origin indicates the SD of the MERRA-2_{TCO}. In the WH region, it is seen that both products have a good correlation (0.8) and a low RMS (4.6) during DJF, MAM, JJAS, and ON seasons. Whereas in the NE region, the correlation coefficient ranges from 0.90 to 0.97 with a high correlation (0.97) and low RMS (~ 3.5) during the MAM season. In the NW region, seasonal correlation varies from 0.4 to 0.9), and the highest correlation coefficient between both datasets is obtained during the DJF season (0.9) with a low RMS value of 4.0. Over southern regions, the correlation coefficient ranges from − 0.1 (SPI) to 0.9 (WPI). In the EPI and SPI regions, both the products show a good correlation during the MAM season with a correlation of 0.8, while in the WPI region, a good correlation is seen in the DJF season (0.9).

Overall, according to the statistics of four seasons, the MERRA-2_{TCO} is in better agreement with AIRS, especially in winter and pre-monsoon seasons. During the winter, columnar ozone from both datasets is highly matched across northern India (WH, NE, NW, and NC). Whereas in southern India (EPI, WPI, and SPI) high correlation is seen during the pre-monsoon season followed by the winter season.

Regional variation of total column ozone

The Violine plot in Fig. 10 depicts the MERRA-2 & AIRS retrieved long-term (2009–2020) average TCO over the selected study region. To visualize data distributions and their probability density, a combination of box plots and density charts is utilized (Hintze and Nelson 1998), where the thick black bar in the middle indicates the interquartile range and the middle white bar denotes the median value. In the NE region, $AIRS_{TCO}$ and $MERRA2_{TCO}$ lie in the range of 200–310 DU and 210–350 DU, respectively, with maximum ozone occurring in an approximately 260–290 DU value range. The TCO distribution in the WH region is 199–420 DU (AIRS) and 230–420 DU (MERRA-2), with a low probability density above 350 DU. In addition, TCO is higher in the NW and NC regions. Additionally, TCO is spread in the 210–340 DU(AIRS) and 240–350 DU(MERRA-2) value ranges in the NW and NC regions. Comparatively columnar ozone is spread in a modest range in southern regions (EPI, WPI, and SPI), i.e., 230–290 DU (MERRA-2) and 210–320 DU (AIRS), with the greatest density being approximately 280 DU roughly.

The column graph (bottom panel (Fig. 10)) represents the comparative analysis of both the products for different regions of India. It is seen that MERRA-2 average TCO is

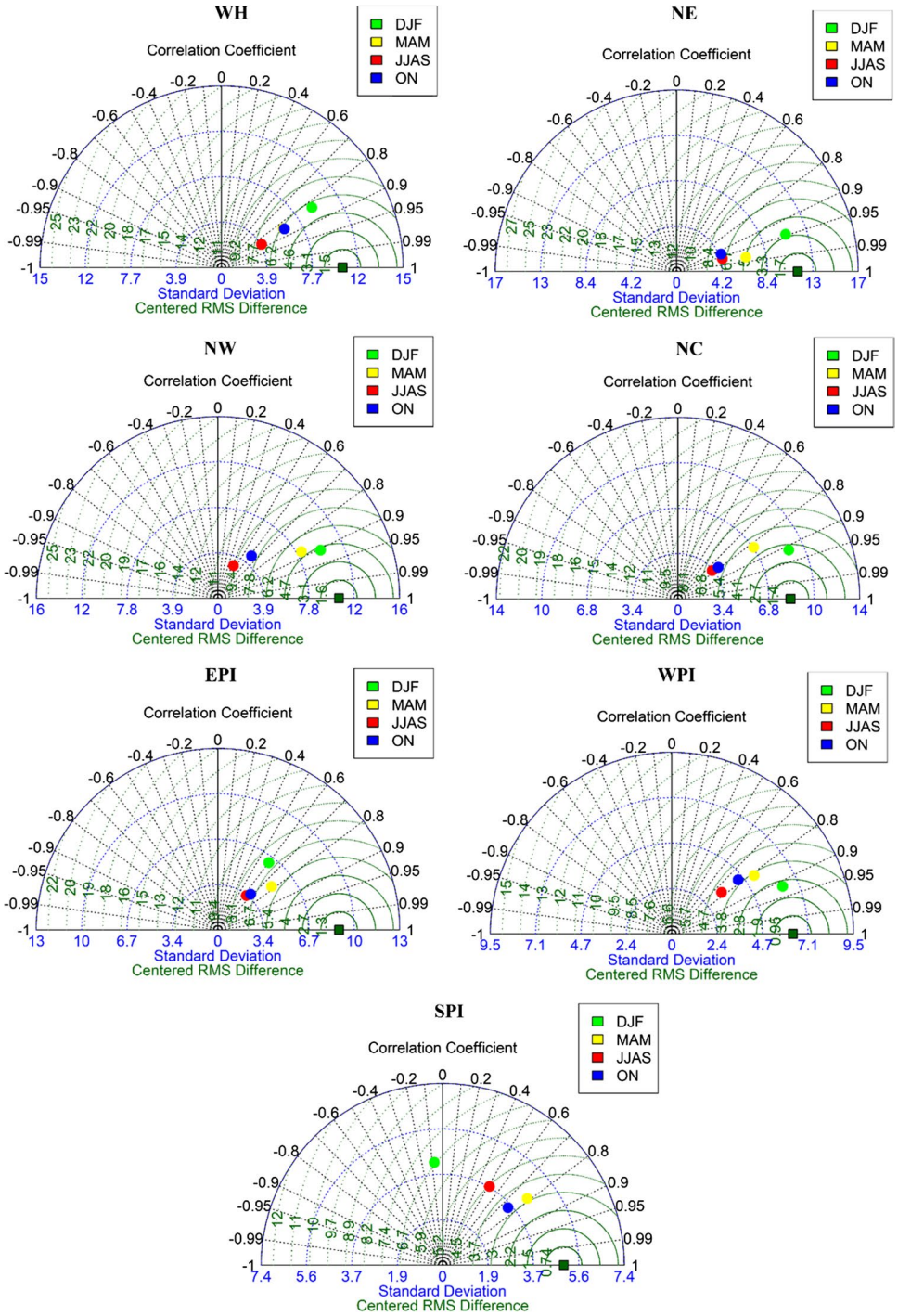

Fig. 9 Taylor diagrams of seasonal TCO, comparing MERRA-2 reanalysis with AIRS satellite in different regions of India for the period 2009–2020

high in almost all the regions except WPI and EPI. In the EPI region, $AIRS_{TCO}$ lies in close proximity to $MERRA2_{TCO}$ with a slight overestimation of the MERRA-2 reanalysis dataset by + 0.6 DU. While in the WPI region, a high average $AIRS_{TCO}$ is obtained compared to $MERRA2_{TCO}$. This significant variation in columnar ozone measurements between MERRA-2 and AIRS is probably caused by topography or surface characteristics, such as land, desert, snow, or ice. Furthermore, region-wise comparative analysis reveals high 12-year TCO in the WH region, i.e., 277 DU (AIRS) and 300 DU (MERRA-2), followed by the NW region (AIRS (272 DU), MERRA-2 (282 DU)), and the NC region (NOAA). While in the southern region, high TCO is obtained over the WPI region (AIRS = 272 DU, MERRA-2 = 270 DU),

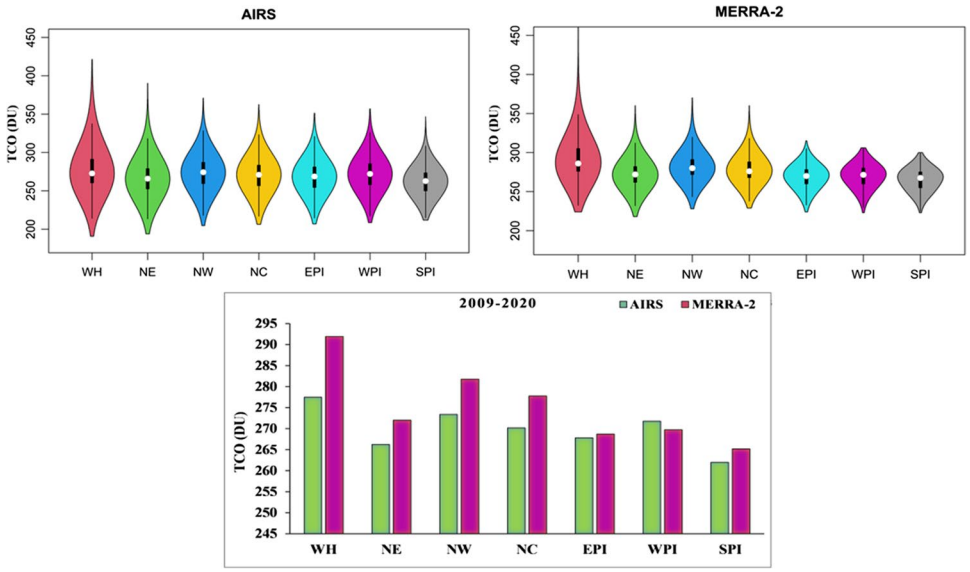

Fig. 10 Twelve year (2009–2020) average TCO over different regions of India (WH, NE, NW, NC, WPI, EPI, and SPI)

followed by the EPI and SPI regions. Overall, it is seen that average TCO gradually increases from low to high latitude, i.e., from SPI (263–266 DU) to WH regions of India (277–300 DU).

Discussion and conclusion

Comparative analysis of MERRA-2 columnar ozone with IMD observed and AIRS satellite datasets reveals that MERRA-2 is a righteous tool for temporal and spatial TCO study. In the current paper, the MERRA-2 columnar ozone is systematically evaluated and validated with ground-based and AIRS satellite products over the Indian regions. Long-term (2009–2020) evaluation with ground-based datasets over Delhi and Varanasi cities shows good agreement of the MERRA-2 product with low NMSE, FB, and high R, d values. The results of simple linear regression analysis show a positive TCO trend value of 0.31% and 0.44% per decade in Delhi and Varanasi, respectively. This increasing trend might be due to increasing anthropogenic activities. Furthermore, a comparative analysis of MERRA-2 with AIRS has been undertaken for seven regions (WH, NE, NW, NC, EPI, WPI, and SPI) in India on a daily, monthly, annual, and seasonal basis. The seasonal variation of columnar ozone shows maximum TCO concentration (305–315 DU) during the summer months, i.e., March, April, and May for all regions of India except WH. The spatial variation of annual average TCO in both datasets (MERRA-2 and AIRS) shows an almost identical distribution pattern, ranging from 270 to 284 DU in the northern regions (WH, NE, NW, and NC) to 260 to 274 DU in the southern regions (WPI, EPI, and SPI) of India. Furthermore, the TCO distribution seems to show significant variability with different seasons and topography. The seasonal spatial pattern displays that high TCO concentrations are associated with high temperatures and sunshine hours during the summer season (MAM). While low TCO is observed in the winter season (DJF) owing to less photochemical production during the cold season. Furthermore, depending on seasons, MERRA-2_{TCO} differs slightly from $AIRS_{TCO}$. During the winter and pre-monsoon seasons, MERRA-2 seems to be overestimated by (+ 1 to + 8 DU) almost in all the regions, while during the monsoon and post-monsoon, MERRA-2TCO is highly underestimated (by − 8 to − 1 DU). Furthermore, 12 years of (2009–2020) annual variations of average TCO show MERRA-2 and AIRS follow the same trends with large data differences in the WH region and low data differences in the EPI and SPI regions. Finally, region-wise comparison illustrates a good agreement between MERRA-2_{TCO} and $AIRS_{TCO}$ products, with NMSE values ranging from 0.0023 (WPI) to 0.0047 (WH) and FB of 0.05(WH) to − 0.0075 (WPI). In support of Brewer's circulation pattern, an increasing shift of columnar ozone from low (SPI) to high (WH) latitudinal regions is also seen from both the datasets.

Appendix 1

Comparison statistics

The statistical tools used to evaluate the MERRA-2_{TCO} comprise the normalized mean square error (NMSE), fractional bias (FB), correlation coefficient (r), index of agreement (d), and a fraction of model predictions within a factor of two of observation (FA2) which are given by following equations.

$$\mathrm{NMSE} = \frac{\left(\mathbf{X_M} - \mathbf{X_O}\right)^2}{\overline{\mathbf{X}}_\mathbf{M}\overline{\mathbf{X}}_\mathbf{O}} \tag{1}$$

$$\mathrm{FB} = \frac{\left(\overline{\mathbf{X}}_\mathbf{M} - \overline{\mathbf{X}}_\mathbf{O}\right)}{0.5\left(\overline{\mathbf{X}}_\mathbf{M} + \overline{\mathbf{X}}_\mathbf{O}\right)} \tag{2}$$

$$\mathrm{R} = \frac{\left(\mathbf{X_O} - \overline{\mathbf{X}}_\mathbf{O}\right)\left(\mathbf{X_M} - \overline{\mathbf{X}}_\mathbf{M}\right)}{\boldsymbol{\sigma}_{\mathbf{X_M}}\boldsymbol{\sigma}_{\mathbf{X_O}}} \tag{3}$$

FA2=Fraction of data which satisfy

$$0.5 \le \frac{\mathbf{X_M}}{\mathbf{X_0}} \le 2.0 \tag{4}$$

$$\mathrm{d} = 1 - \frac{\sum_{\mathbf{i}=1}^{\mathbf{n}}\left(\mathbf{X_{O_i}} - \mathbf{X_{M_i}}\right)^2}{\sum_{\mathbf{i}=1}^{\mathbf{n}}\left(\left|\mathbf{X_{M_i}} - \overline{\mathbf{X}}_\mathbf{O}\right| + \left|\mathbf{X_{O_i}} - \overline{\mathbf{X}}_\mathbf{O}\right|\right)^2} \tag{5}$$

where:

X_M MERRA-2_{TCO}

X_o observations/$AIRS_{TCO}$

$\overline{X}_O$ and $\overline{X}_M$ average of the dataset

σ_{X_M} and σ_{X_O} standard deviation of the dataset

Simple linear regression (SLR) for TCO trend analysis

Trend analysis is used to study the TCO variation with respect to time. We have used simple linear regression (SLR) to compute the trend in the original time series of the TCO dataset for long-term period of 2009–2018.

Table 3 Evaluation of AIRS against IMD

Statistics	AIRS Vs. IMD	
	Delhi	Varanasi
NMSE	0.0042	0.0052
R	0.73	0.66
FB	0.019	0.012
FA2	100	100
D	0.83	0.77

Monthly mean TCO data were derived from the IMD and MERRA-2 daily product. A linear regression statistical model is expressed as:

$$\mathbf{X} = \mathbf{a} \times \mathbf{t} + \mathbf{c} \tag{6}$$

where:

X monthly mean TCO.

a slope coefficient in linear regression line.

t time period in months.

c intercept.

The least squares method (LSM) is used to determine the regression coefficients *a* and *c* to minimize the residual sum of squares (Jain et al. 2008; Toihir et al. 2018; Potdar et al. 2018). The trend variation is calculated in % DU per decade by the equation:

$$\frac{\mathbf{a} \times 10 \times 12}{\mathbf{AvgTCO}} \times 100 \tag{7}$$

Here, a slope coefficien.

Avg_{TCO} average TCO value for the selected period.

Table 3

Acknowledgements MERRA-2 data is obtained from https://gmao.gsfc.nasa.gov/reanalysis/MERRA-2/data_access/. AIRS data were obtained from Level-2, (https://disc.gsfc.nasa.gov/datasets/AIRS2RET_006/summary?keywords=airs%20version%207). We also acknowledge the AIRS mission scientists, Worldview, and associated NASA personnel for the production of the data used in this research effort. We also acknowledge the data from the Indian Meteorological Department (IMD), India.

Author contribution The first author Priyanshu Gupta drafted the methodology and validation analysis. Dr. Sunita Verma conceptualized the work by drafting the initial manuscript taken up by Priyanshu. Ms. Priyanshu Gupta did the initial data collection, graphics, format

analysis, and visualization. Prof. R. Bhatla and Dr. Swagata investigated and supervised overall work at different stages.

Funding The funding support from the Ministry of Earth Sciences (MoES/16/18/2017-RDEAS), Government of India, is acknowledged.

Data availability All the data sets used in this present study are available publicly and the same has been provided in the manuscript as well as in the "Acknowledgements" section.

Declarations

Ethical approval Authors consciously assure that the manuscript is an original work and follows the ethical standards of research.

Consent to participate Not applicable.

Consent for publication Not applicable.

Competing interests The authors declare no competing interests.

References

Aumann HH, Chahine MT, Gautier C, Goldberg MD, Kalnay E, McMillin LM, Susskind J (2003) AIRS/AMSU/HSB on the aqua mission: design, science objectives, data products, and processing systems. IEEE Trans Geosci Remote Sens 41(2):253–264

Bosilovich M et al (2015) MERRA-2: initial evaluation of the climate. NASA technical report series on global modeling and data assimilation, NASA/TM-2015 39:136

Brewer AW (1949) Evidence for a world circulation provided by the measurements of helium and water vapour distribution in the stratosphere. Q J R Meteorol Soc 75(326):351–363

Butchart N (2014) The brewer-dobson circulation. Rev Geophys 52(2):157–184

Chakrabarty DK, Peshin SK (1997) Behavior of ozone over Indian region after Pinatubo eruption. J Geophys Res: Atmos 102(D5):6153–6157

Chakrabarty DK, Peshin SK, Pandya KV, Shah NC (1998) Long-term trend of ozone column over the Indian region. J Geophys Res: Atmos 103(D15):19245–19251

Chipperfield MP, Bekki S, Dhomse S, Harris NR, Hassler B, Hossaini R, Weber M (2017) Detecting recovery of the stratospheric ozone layer. Nature 549(7671):211–218

Cohn SE (1997) An introduction to estimation theory (gtspecial issueltdata assimilation in meteology and oceanography: theory and practice). J Meteorol Soc Japan Ser II 75(1B):257–288

Crutzen PJ (1974) Photochemical reactions initiated by and influencing ozone in unpolluted tropospheric air. Tellus 26(1–2):47–57

de Forster F, Piers M, Shine KP (1997) Radiative forcing and temperature trends from stratospheric ozone changes. J Geophys Res: Atmos 102(D9):10841–10855

Divakarla M, Barnet CD, Goldberg MD, McMillin LM, Maddy E, Wolf W, Zhou L, Liu X (2006) Validation of atmospheric infrared sounder temperature and water vapor retrievals with matched radiosonde measurements and forecasts. J Geophys Res 111:D09S15. https://doi.org/10.1029/2005JD006116

Fioletov VE (2008) Ozone climatology, trends, and substances that control ozone. Atmos Ocean 46(1):39–67

Gupta P, Verma S, Bhatla R, Chandel AS, Singh J, Payra S (2020) Validation of surface temperature derived from MERRA-2 reanalysis against IMD gridded data set over India. Earth and Space Science 7(1):e2019EA000910

Han Z, Chongping J, Libo Z, Wei W, Yongxiao J (2001) ENSO signal in total ozone over Tibet. Adv Atmos Sci 18(2):231–238

Hintze JL, Nelson RD (1998) Violin plots: a box plot-density trace synergism. Am Stat 52(2):181–184

Jain SL, Kulkarni PS, Ghude SD, Polade SD, Arya BC, Dubey PK (2008) Trend analysis of total column ozone over New Delhi, India. MAPAN. Journal Metrology Society of India 23:63–69

Kalnay E (2003) Atmospheric modeling, data assimilation and predictability. Cambridge University Press

Kim S, Park SJ, Lee H, Ahn DH, Jung Y, Choi T, Koo JH (2021) Evaluation of total ozone column from multiple satellite measurements in the antarctic using the brewer spectrophotometer. Remote Sens 13(8):1594

Kleist DT, Parrish DF, Derber JC, Treadon R, Errico RM, Yang R (2009) Improving incremental balance in the GSI 3DVAR analysis system. Mon Weather Rev 137(3):1046–1060

Komhyr WD, Evans RD (1980) Dobson spectrophotometer total ozone measurement errors caused by interfering absorbing species such as SO2, NO2, and photochemically produced O3 in polluted air. Geophys Res Lett 7(2):157–160

Komhyr WD, Grass RD, Leonard RK (1989) Dobson spectrophotometer 83: a standard for total ozone measurements, 1962–1987. J Geophys Res: Atmos 94(D7):9847–9861

Lal S, Venkataramani S, Srivastava S, Gupta S, Mallik C, Naja M, ..., Liu X (2013) Transport effects on the vertical distribution of tropospheric ozone over the tropical marine regions surrounding India. J Geophys Res: Atmos 118(3):1513–1524

Lefohn AS, Malley CS, Smith L, Wells B, Hazucha M, Simon H, ..., Lewis A (2018) Tropospheric ozone assessment report: global ozone metrics for climate change, human health, and crop/ecosystem research. Elementa: Sci Anthropocene 6

Legates DR, McCabe GJ Jr (1999) Evaluating the use of "goodness-of-fit" measures in hydrologic and hydroclimatic model validation. Water Resour Res 35(1):233–241

Londhe AL, Bhosale CS, Kulkarni JR, Kumari BP, Jadhav DB (2003) Space-time variability of ozone over Indian region for the period 1981–1998. J Geophys Res 108(D24):8781. https://doi.org/10.1029/2002JD002942

Lu X, Zhang L, Liu X, Gao M, Zhao Y, Shao J (2018) Lower tropospheric ozone over India and its linkage to the South Asian monsoon. Atmos Chem Phys 18(5):3101–3118

McConnell JC, Jin JJ (2008) Stratospheric ozone chemistry. Atmos Ocean 46(1):69–92

McFarlane N (2008) Connections between stratospheric ozone and climate: radiative forcing, climate variability, and change. Atmos Ocean 46(1):139–158

Monahan KP, Pan LL, McDonald AJ, Bodeker GE, Wei J, George SE, Barnet C, Maddy ES (2007) Validation of AIRS v4 ozone profiles in the UTLS using ozonesondes from Lauder, NZ and Boulder, USA. J Geophys Res 112:D17304. https://doi.org/10.1029/2006JD008181

Pathakoti M, Santhoshi T, Aarathi M, Mahalakshmi DV, Kanchana AL, Srinivasulu J, ..., Raja P (2021) Assessment of spatio-temporal climatological trends of ozone over the Indian region using machine learning. Spat Stat 43:100513

Potdar SS, Nade DP, Pawar RP, Victor NJ, Nikte SS, Chavan GA, Taori A, Singh D (2018) Statistical analysis of total column ozone during three recent solar cycles over India. J Atmos Sol Terr Phys 181:44–54. https://doi.org/10.1016/j.jastp.2018.10.015

Randel WJ (1988) The seasonal evolution of planetary waves in the Southern Hemisphere stratosphere and troposphere. Q J R Meteorol Soc 114(484):1385–1409

Resmi CT, Nishanth T, Vijoy PS, Kumar MS, Balachandramohan M (2020) Analysis of long-term variation of the total column

and tropospheric ozone over the Indian region. Atmos Clim Sci 11(1):194–213
Sahoo A, Sarkar S, Singh RP, Kafatos M, Summers ME (2005) Declining trend of total ozone column over the northern parts of India. Int J Remote Sens 26(16):3433–3440
Salby M, Titova E, Deschamps L (2011) Rebound of Antarctic ozone. Geophys Res Lett 38:L09702. https://doi.org/10.1029/2011GL047266
Shepherd TG (2008) Dynamics, stratospheric ozone, and climate change. Atmos Ocean 46(1):117–138
Soni VK, Pandithurai G, Pai DS (2012) Evaluation of long-term changes of solar radiation in India. Int J Climatol 32(4):540–551
Susskind J, Barnet C, Blaisdell J, Iredell L, Keita F, Kouvaris L, Molnar G, Chahine M (2006) Accuracy of geophysical parameters derived from AIRS/AMSU as a function of fractional cloud cover. J Geophys Res 111:D09S17. https://doi.org/10.1029/2005JD006272
Susskind et al (2011) Improved temperature sounding and quality control methodology using AIRS/AMSU data: the AIRS science team version-5 retrieval algorithm. IEEE Trans Geosci Remote Sens 49:883–907. https://doi.org/10.1109/TGRS.2010.2070508
Tandon A, Attri AK (2011) Trends in total ozone column over India: 1979–2008. Atmos Environ 45(9):1648–1654
Toihir AM, Portafaix T, Sivakumar V, Bencherif H, Pazmino A, Begue N (2018) Variability and trend in ozone over the southern tropics and subtropics. Ann Geophys 36:381–404. https://doi.org/10.5194/angeo-36-381-2018
Wargan K, Pawson S, Olsen MA, Witte JC, Douglass AR, Ziemke JR, Nielsen JE (2015) The global structure of upper troposphere-lower stratosphere ozone in GEOS-5: a multiyear assimilation of EOS Aura data. J Geophys Res: Atmos 120(5):2013–2036
Weber M, Dikty S, Burrows JP, Garny H, Dameris M, Kubin A, Langematz U (2011) The Brewer-Dobson circulation and total ozone from seasonal to decadal time scales. Atmos Chem Phys 11(21):11221–11235
Ziemke JR, Oman LD, Strode SA, Douglass AR, Olsen MA, McPeters RD, Taylor SL (2019) Trends in global tropospheric ozone inferred from a composite record of TOMS/OMI/MLS/OMPS satellite measurements and the MERRA-2 GMI simulation. Atmos Chem Phys 19(5):3257–3269